P4.3 RADAR AND DAMAGE ANALYSIS OF BOW ECHOES OBSERVED DURING BAMEX

Dustan M. Wheatley* and Robert J. Trapp
Purdue University, West Lafayette, Indiana

Nolan T. Atkins
Lyndon State College, Lyndonville, Vermont

1. INTRODUCTION

Straight-line winds that accompany bow echoes can cause significant damage in the United States and elsewhere. Our physical understanding of the mechanisms that produce severe winds within bow echoes is the culmination of several inquiries in severe storms research. Early studies by Nolen (1959) and Hamilton (1970) recognized the severe weather potential of bulging radar-echo configurations. Fujita (1978) provided the first conceptual representation of the structure and evolution of severe bow echoes. In Fujita's conceptual model, as considered from a radar perspective, a strong, tall echo transitions to a bow echo under the influence of intense downdrafts near the bow-echo apex. Later studies (Smull and Houze 1987; Jorgensen and Smull 1993) further clarified the kinematic structure of bow echoes by documenting the presence of a midlevel, rear-inflow jet. Descending rear inflow at the bow-echo apex has been generally accepted as the primary source of damaging winds near the ground.

Recent idealized numerical simulations, though, suggest an evolving conceptualization of damaging wind production in bow echoes. Specifically, Trapp and Weisman (2003) found that the *most* damaging winds in mature, extensive bow echoes can occur tens of kilometers northwest of the bow-echo apex. These damaging surface winds are induced by large horizontal pressure gradients associated with low-level meso-g-scale (approx. 2-20 km diameter; Orlanski 1975) vortices, or "mesovortices," along the leading edge of the convective system. Notably, the wind damage pattern associated with these vortices would be "straight-line" in appearance, a consequence of their size and asymmetry.

* *Corresponding author address:* Dustan M. Wheatley, Dept. of Earth and Atmospheric Sciences, Purdue University, West Lafayette, IN 47906; email: dwheatle@purdue.edu

As found in the simulations, mesovortices are especially favored in environments characterized by moderate to strong low-level unidirectional vertical wind shear ($\geq$15 J kg^{-1} over the lowest 2.5 km AGL) and large instability (e.g., CAPE greater than approximately 2000 J kg^{-1}; Weisman and Trapp 2003). Under these conditions, the midlevel RIJ remains elevated until bifurcating near the leading edge of the system, which confines RIJ-associated winds to a narrow band in proximity to the apex. Thus, the numerical results suggest that mesovortex winds can be more extreme, have longer duration, and (instantaneously) affect a larger area than RIJ/apex winds. Bow echoes simulated in weaker shear regimes possess weaker, shorter-lived mesovortices.

Mesovortices are observed frequently (e.g., Funk et al. 1999); however, the corroborative observational data that clearly differentiates low-level mesovortex from RIJ-associated winds is limited. At present, only a few observational studies in the informal literature have indirectly or directly documented the role of mesovortices in the production of damaging surface winds within bow echoes. Miller and Johns (2000) investigated several long-lived mesoscale convective systems (MCSs) that produced what they referred to as "extreme" damaging wind, tantamount in this case to upper-F1 intensity damage. One such system, a bow echo event on 4 July 1999, caused a widespread tree blowdown in northern Minnesota. Markedly, this wind damage occurred beneath what they referred to as a super cell embedded within the northern flank of the system. Wind damage in proximity to the apex was less dense, with only pockets of extreme wind damage.

Wolf's (2000) analysis of the early formation of the bow-echo event on 29 June 1998 revealed six subsystem-scale, cyclonic vortices along the leading edge of the convective system, five of which were tornadic. All of the vortices formed in proximity to or north of the bow-echo apex, and were in general short-lived (lasting only a few volume scans). While the convective event produced widespread, F0-intensity wind damage across eastern Iowa and central Illinois, localized swaths of F1-intensity wind damage were found to occur in association with the cores of the nontornadic circulations. Similar relations between vortex tracks and point observations were noted by Pryzbylinski et al. (2000) and Schmocker et al. (2000). Finally, Cotton et al. (2003) suggested an indirect role of midlevel vortices in the production of damaging straight-line winds.

The results of the studies summarized above indicate the need to revisit the established model and delve deeper into hypothesized ideas of damaging wind production within bow echoes. Indeed, the data needed to systematically do so have recently become available through the auspices of the Bow Echo and MCV Experiment (BAMEX; Davis 2004). Specifically, detailed poststorm damage surveys were conducted during the BAMEX field phase and provide the dataset necessary to begin this investigation. Our objectives herein are to:

1. elucidate where damaging surface winds occurred within the bow-shaped convective system (in proximity to the apex, north of the apex, etc.), and then

2. explain the existence of these winds in the context of the theorized mechanisms (mesovortices, RIJ, etc.).

In section 2, the data sources are described, followed by a discussion of the research methodology employed in this study. In sections 3-6, each of six bow-echo events is then described in detail. Damage analyses and complementary radar-damage analyses of each event are presented in order to determine the mechanism(s) of damaging wind production. Finally, in section 7, the results of this study are summarized, their implications are discussed, and suggestions for future research on this topic are offered.

2. METHODOLODY

This study examines the possible mechanism(s) of damaging wind production in six bow-echo events observed during the BAMEX field phase; Table 1 provides a summary of these BAMEX events. The project dates for BAMEX were 20 May - 6 July 2003, a period when severe bow echoes are climatologically favored. The experimental domain over which operations were conducted encompassed the Midwest, Upper Ohio Valley and parts of the Great Plains, where the spatial distribution of severe bow echo events is most significant. Although a number of special airborne and ground-based observing instruments were deployed during BAMEX (see Davis 2004), our two objectives required only post-event damage surveys and the existing network of WSR-88D radars.

2.1 *Damage Survey Techniques*

Detailed aerial and ground surveys of wind damage were conducted by the authors and other BAMEX personnel (see Table 1) immediately following apparently severe bow echo events. Because conventional surface observations are sparse relative to the scale of damaging winds, these surveys were critical in "defining" the near-surface wind field within severe bow echoes. Further, while *Storm Data* reports (damage locations, estimates of property damage, etc.) are routinely cited in studies that investigate the severe weather elements that occur in association with severe convective storms, uncertainties in this dataset largely (although not wholly) preclude the fusion of this information into the present study. Indeed, as a source of verification, Witt et al. (1998) found that *Storm Data* reports are often incomplete and inaccurate.

The scope of ground and aerial surveys was guided by initial storm reports to National Weather Service (NWS) offices and also by Doppler radar imagery. For most events that occurred over an expansive geographic area, aerial surveys were flown using Cessna aircraft to photo-document the scale and intensity of the wind damage. This type of survey facilitated the most comprehensive post-event assessment of the low-level wind field within a severe bow echo, and provided "right of entry" to those areas (private property, etc.) inaccessible from the existing road network. Further, aerial surveying was advantageous in discerning convergence/divergence patterns associated with tornadic and "straight-line" winds, respectively. For completeness, a ground survey team also was deployed immediately following bow echo events of interest. While this type of survey was constrained by the existing road network, it often yielded information about damage intensity that was not evident from the air.

It should be noted that even these special surveys have limitations. As stated, initial survey efforts focused primarily on the areas highlighted in the first storm reports to NWS offices. Expanded survey efforts followed from assessment of these areas, so it is conceivable that unreported damage areas failed to be included in this study. Nonetheless, for reasons already discussed, this approach was favored over a complete dependence upon *Storm Data* reports.

All damage locations were superimposed on high-resolution (1:250,000) U.S. Geological Survey (USGS) topographic maps. "Damage vectors" were used to denote the direction of tree fall and/or the direction in which structural damage was strewn. In some instances, a direction could not be determined due to cleanup efforts that occurred in the days following the severe winds; these damage locations were denoted simply with a point. Variations of this convention are otherwise noted on a case-by-case basis.

The damage information collected during each survey effort was synthesized into a comprehensive damage analysis, which provides a quantitative description of the scale and intensity of the wind damage. Similar to damage analyses of isolated tornadic thunderstorms, the observed wind speed at each location was assessed in accordance with the Fujita damage intensity scale.

2.2 *Single-Doppler Radar Data*

The radar data used in this study were obtained from the National Climatic Data Center (NCDC) WSR-88D Archive Level II data set, comprised of reflectivity, mean radial velocity, and spectrum width over full volumetric scans. Single-Doppler radar observations were incorporated in the present study from the following WSR-88D sites across the Midwest: Des Moines, IA (KDMX); Wilmington, OH (KILN); Indianapolis, IN (KIND); North Webster, IN (KIWX); and Omaha, NE (KOAX). For diagnostic purposes, the WSR-88D radar data had to be preprocessed (using the software program Solo; Oye et al. 1995) for velocity dealiasing, as the Doppler velocity measurements were oftentimes ambiguous.

To ensure an accurate comparison between geographic locations defined by the radar data and surveys, it was highly desirable to check the accuracy of range and azimuth measurements of these single-Doppler radar data sets. This was accomplished using fixed ground targets (radio towers, water towers, etc.) of known locations (Rinehart 1978). Such non-meteorological targets were identified in Doppler radial velocity data as a consequence of their immobility, and were often also represented on U.S. Geological Survey topographic maps. The distance and azimuth of a target were then measured directly on the map and compared with those values obtained from the radar data, from which a correction factor was derived. No significant offsets were found in any of the radar data.

2.3 *Radar and Damage Analysis*

Images of each damage survey were coupled with radar imagery of the BAMEX event. This simple technique has been employed in published studies of isolated tornadic storms and hurricanes (e.g., Wakimoto and Atkins 1996; Wakimoto and Black 1994), but its utility in studies of quasi-linear convective systems has yet to be fully realized.

Analogous to the supercell mesocyclone, mesovortices were identified in Doppler wind field as a velocity couplet, or adjacent maxima of radial velocities of opposite sign. As such, the Mesocyclone Detection Algorithm (MDA) included in the research version of Warning Decision Support System – Integrated Information (WDSS-II; Lakshmanan 2002; Stumpf et al. 2002) was utilized in the current study to facilitate the identification of these circulation features. Other information derived from the MDA includes the center (i.e., azimuth/range), base/depth, low-level diameter, low-level rotational velocity, maximum rotational velocity, and direction/speed of all relevant three-dimensional shear regions. The RIJ was typically identified as a maximum of rear-to-front flow behind the convective line. This information, once merged with damage information, allowed us to make associations between the scale and intensity of the wind damage and radar-observed structural characteristics (mesovortices, RIJ, etc.) of the bow echo.

3. WINGATE, INDIANA: 31 MAY 2003

During this event, a line of supercells (of approximately 30-km spacing) developed ahead of a strong cold front over southern Wisconsin. As the line propagated into northern/central Illinois and Indiana, it evolved into an intense MCS that persisted for several hours. The primary focus of this analysis is a nearly S-shaped segment of convective cells over portions of central Indiana. During the period 03:15:12 – 03:35:07 UTC, a shallow, broad (order 5-10 km) mesovortex was observed along the leading edge of the MCS.

As one might expect based upon its size and structure (see Figure 1a), this MCS was not a prolific producer of nontornadic wind damage. Preliminary severe weather reports indicated that most of the wind damage resulted from tornadoes that occurred over central/northern Illinois. Nevertheless, detailed aerial and ground surveys following this event revealed a localized swath of F0-intensity wind damage approximately 15 kilometers in length, centered about the town of Wingate, Indiana (Fig. 1a).

This damage area has been superimposed on the KIND radar reflectivity display at 03:29:49 UTC to establish the spatial correlation between convective system structure and the damage locations. At this time, a shallow, broad mesovortex was observed in Doppler winds on the 0.5-degree elevation surface (approximately 1.5 km ARL). This circulation persisted over 5 volume scans (approximately 25 minutes), as indicated by the track of the vortex core in Fig. 1b. Throughout its lifetime, the mesovortex showed no tendency to build upward, as its vertical depth was confined to the lowest elevation surface.

The onset of damaging surface winds occurred around 03:24:50 UTC and persisted for three volume scans. During this period, winds on the southern periphery of the vortex core coincided with the observed wind damage (Fig. 1b). By 03:40:06 UTC, no circulation could be detected in Doppler winds and damaging surface winds had ceased.

4. EASTERN NEBRASKA: 10 JUNE 2003

This high wind event featured a mature, extensive bow echo that evolved from two cell bow echoes, which in turn evolved from two tornadic supercells over eastern Nebraska. The first supercell to bow echo evolution occurred over northeastern Nebraska around 0100 UTC, and a similar evolutionary mode was observed over east-central Nebraska around 0300 UTC. In each case, the transition process occurred rather rapidly (less than 30 minutes), and damaging wind production was confined to the early formation of the bow echo. Both isolated, smaller-scale bow echoes exhibited rapid upscale growth over the next several hours before merging into a larger-scale bow echo over southwestern Iowa. This system continued to propagate toward the southeast and affected the Greater St. Louis, Missouri area around 1200 UTC. BAMEX observations (airborne Doppler radar data) documented the presence of rear-inflow in the trailing stratiform precipitation region at this time; however, an aerial survey conducted post-event found that this larger-scale bow echo produced relatively minor damage as it moved through Missouri. Thus, this analysis focuses primarily on the two smaller-scale bow echoes that did, in fact, produce damaging winds at the ground.

4.1 *"Emerson" Bow Echo*

Aerial and ground surveys conducted in the days immediately following this bow echo event revealed a swath of concentrated F0-intensity wind damage approximately 40 km in length (Fig. 2). The most significant wind damage occurred in Emerson, Nebraska and surrounding areas, where severe winds caused widespread tree and power line damage, as well as minor structural damage. Property damage in these areas was estimated at $100,000 *(Storm Data).*

The movement of the Emerson bow echo over the period 01:17:45 - 01:47:45 UTC (as depicted by KOAX radar reflectivity displays) is of primary interest to this analysis. At 01:17:45, the apex of an intense cell bow echo was nearly coincident with the first damage locations (not shown). Indeed, radial velocity data on the 0.5-degree elevation surface depicted a narrow RIJ that extended tens of kilometers behind the leading edge of the system (not shown). This radar echo configuration was observed at each subsequent analysis time, as the RIJ/apex winds remained nearly collocated with the damage area as the system propagated toward the southeast (e.g., Figs. 3a-b). During this period, the convective system exhibited rapid bowing. At 01:47:45 UTC, a 40-km-wide horseshoe-shaped segment of convective cells was depicted in radar reflectivity (not shown), although this system was no longer producing damaging surface winds.

4.2 *"Shelby" Bow Echo*

In east-central Nebraska, survey efforts also revealed a rather narrow swath of F1-intensity wind damage approximately 10 km in length embedded within a broader distribution of F0-intensity damage locations approximately 30 km in length (Fig. 4). A secondary area of F1-intensity wind damage appeared to be the consequence of microburst winds, owing to the largely divergent flow implied by the orientation of the damage vectors. Property damage in Shelby, Nebraska alone was estimated at one million dollars *(Storm Data)*. In addition, twenty-two irrigation systems were overturned throughout the damage area, several of which appeared to have been rolled over twice. It is interesting to note here that initial storm reports to the NWS mentioned only tree damage north of Shelby.

Similar to the previous analysis, RIJ/apex winds were likely the primary mode of damaging wind production in the Shelby bow echo. At 03:02:59 UTC, the first F0-intensity damage locations lay underneath the apex of a 20-km-wide cell bow echo (not shown). Corresponding radial velocity data showed an intense RIJ that extended tens of kilometers rearward of the system's leading edge (not shown). At subsequent analysis times (e.g., Fig. 5a-b), a narrow rear-inflow notch penetrated to the leading edge of the bow-shaped system (just behind the apex), clearly signifying the presence of the RIJ-apex winds.

5. INDIANA/OHIO: 4-5 JULY 2003

The squall-line bow echo on 4-5 July 2003 developed from intense convection over northwest Indiana; the focal point for this convection was a remnant surface outflow boundary, which aided the rapid development of the convective system. A quasi-linear convective system rapidly evolved from this convection, and then moved southeast over central Indiana and eastern Ohio. The system produced strong surface winds across central Indiana and eastern Ohio, as gauged by *Storm Data* reports (although the relative number of reports could be attributed to the fact that this event occurred on July 4th in late afternoon).

A note of caution accompanies the following damage analysis. No aerial survey of wind damage was performed for this bow echo event, so ground surveys performed over a several day period serve as the observational basis for this case study. Clearly, these efforts were not afforded the “universal” access made possible with aerial surveying. The ground surveys were further complicated by a several-day sequence of convective systems over the same geographic domain affected on 4 July 2003. This resulted in additional tree damage, and also flooding that further limited our access to rural areas. Given these limitations, *Storm Data* reports were used to augment the damage information collected during the ground surveys to provide a more thorough description of the low-level wind field. From our perspective, the consideration of *Storm Data* wind reports seemingly exaggerates the scale and intensity of this bow echo event. The spatial difference between the observed damage area and the tri-state damage area implied by the relatively large number of severe weather reports is unexplained (despite the limitations of the survey efforts).

In central Indiana, survey efforts revealed two areas of relatively dense wind damage (Fig. 6). The first of these damage areas (approximately 20 km in length) was located approximately 40 km east-northeast of the city of Marion, near the Indiana-Ohio border. Several F1-intensity damage locations were observed over central Wells County. The second damage area was a 15-km-long swath of F0 wind damage over parts of Madison and Tipton Counties. Several F1-intensity damage locations also were observed within this broader distribution.

At 22:44:37 UTC, the KIWX radar reflectivity display showed a nearly continuous line of active convection (not shown). A portion of the convective line had assumed an upshear-tilted configuration, as evidenced by an expanding stratiform region on the backside of the system, and developing rear inflow was observed within this stratiform region (not shown). Over the next thirty minutes, the area of rear inflow behind the system’s leading edge increasingly expanded, and the linear disturbance began to bow under its influence (e.g., Figs. 7a-b). Clearly, these RIJ/apex winds were spatially correlated with the observed wind damage over east-central Indiana.

Despite this analysis, it remains unclear which convective system attribute produced the damage area to the northwest of Muncie, Indiana. The KIWX base reflectivity and radial velocity displays at 23:14:24 and 23:14:44 UTC, respectively, showed these damage locations clearly out of phase with the rear inflow in the expanding stratiform region (Figs. 7a-b). The damage area was collocated with an area of weak anticyclonic rotation, and located to the northeast of area of weak cyclonic rotation. From a single-Doppler perspective, neither of these rotational features appeared capable of producing damaging surface winds, but it is possible that their intensities may have been undervalued as the flow inferred from the damage vectors was crossbeam. Although positioned more favorably in terms of range, KIND radar's viewing angle also was orthogonal to the movement of the convective system structure being examined.

The relative severity of the bow echo diminished as it matured and expanded in size; survey efforts only revealed a few pockets of F0-intensity tree damage across southeast Indiana and southwest Ohio. Interestingly, radial velocity data from the KILN radar continued to indicate the presence of a broad area of rear inflow just behind the core of the system. Similar to the early formation of the bow echo, damaging surface winds over southeast Indiana and southwest Ohio were likely driven primarily by RIJ/apex winds.

6. NEBRASKA/IOWA: 5-6 JULY 2003

On 5-6 July 2003, a nocturnal bow echo evolved from intense, convection over southeast

South Dakota and northeast Nebraska, and then moved southeast into western Iowa. This system produced a number of high wind reports, and caused widespread F0-intensity wind damage across eastern Nebraska and western Iowa (*Storm Data)*. This analysis examines damaging wind production within the bow echo on 5-6 July 2003 from early formation to eventual decay.

6.1 *Eastern Nebraska*

In several locations or counties across eastern Nebraska, the number and distribution of damage locations was more significant relative to surrounding areas. Property damage in Osceola, Nebraska alone was estimated at $100,000 (*Storm Data*). Severe winds over eastern Nebraska on 5-6 July 2003 were driven by descending rear-inflow at the bow-echo apex, despite an apparent phase shift between RIJ/apex winds, as depicted in Doppler winds at 04:14:11 UTC (not shown), and the damage area. The orientation of the damage vectors implied a northerly low-level wind field over the affected area, yet the radar viewing angle was orthogonal to this motion. Hence, the scale of the RIJ was not represented in its entirety by radial velocity data.

6.2 Omaha, Nebraska

The bow echo on 5-6 July 2003 produced significant wind damage as it moved through the Omaha metropolitan area (Fig. 8). With its passage, a wind gust of 75 mph was recorded atop a building on the campus of Creighton University (*Storm Data*). A rather narrow swath (approximately 10 km in length) of F0-intensity damage through northern sections of Omaha has been delineated because it exhibited a steep damage gradient, as revealed by an aerial survey. Several F1-intensity damage locations were embedded within this broader distribution. Property damage in Douglas County (the county seat of Omaha) was estimated at two million dollars (*Storm Data*).

At 05:04:03 UTC, the bow-echo apex, as determined by the positioning of the gust front, was located approximately 10 km southeast of the KOAX radar (not shown). In its wake, strong outflow was observed in Doppler winds. Moreover, a cusp in the gust front approximately 10 km northeast of the radar (on the cyclonic shear side of the RIJ) was collocated with a 5-km-wide mesovortex. (Note: Because storm motion exceeded the rotational velocity of the mesovortex, the velocity couplet was manifested in Doppler winds as adjacent maxima of radial velocities of the *same* sign.) Neither structural feature of the bow echo was producing damaging surface winds at this time.

In the subsequent volume scan, Doppler winds again depicted descending rear inflow behind the leading edge of the system and a mesovortex on the cyclonic shear side of the RIJ (not shown). At this time, several damage locations occurred indiscriminately about the position of the mesovortex; however, by 05:14:25, it was no longer possible to detect this circulation feature in radial velocity data.

At 05:24:27 UTC, a mesovortex was once again detected in Doppler winds (Fig. 9b). Mesovortex-induced winds at approximately 1 km above ground level approached 40 $\mathrm{m \cdot s^{-1}}$, and moved directly overhead the only F1-intensity damage locations observed in the Omaha metropolitan area. The spin-up and subsequent decay of this vortical feature occurred rather rapidly, as it could not be identified in the subsequent volume scan.

During this same period, descending rear inflow at the bow-echo apex also produced wind damage in central sections of Omaha. The KOAX radial velocity display 05:24:27 UTC showed the RIJ/apex winds in excess of 35 $\mathrm{m \cdot s^{-1}}$ collocated with numerous F0-intensity damage locations.

6.3 *Western Iowa*

Aerial and ground surveys (by R. Wakimoto) over western Iowa revealed an approximately 50-km-long swath of F0-intensity wind damage occurred across portions of Audubon, Cass, Harrison, Pottawattamie, and Shelby Counties (Fig. 10). An embedded swath (approximately 15 km in length) of F1-intensity wind damage occurred across portions of Harrison and Shelby Counties, where numerous large trees were downed by the severe winds. A secondary area of F0-intensity wind damage, attributed to microburst winds, occurred north of the primary damage area.

At 05:34:09 UTC, an undulation in the steep reflectivity gradient at the leading edge of the system indicated the presence of an incipient mesovortex (not shown). Corresponding radial velocity data showed weak rotation on the lowest elevation scan collocated with this redistribution of the rainwater field (not shown). This circulation was located tens of kilometers north of the apex, as determined from the gust front's orientation.

Over the next five minutes, the mesovortex experienced rapid intensification, and by 05:39:30 UTC, winds on the southern periphery of its core were producing F0-intensity wind damage over parts of southeast Harrison County (see Fig. 11b). On a time-scale less than one volume scan, mesovortex-induced winds reached peak intensity, as evidenced by the steep damage gradient between unaffected areas and the first F1-intensity damage locations. From an airborne Doppler analysis of this event (not part of the current study), we know that near-surface winds were at times around 40 $\mathrm{m \cdot s^{-1}}$. The most damaging winds associated with BEV2 continued over the duration of the next two volume scans.

A pronounced hook-like structure was observed in radar reflectivity at 05:54:13 UTC in association with the mesovortex (Fig. 11a), which was depicted in Doppler winds as an approximately 5-10-km-wide velocity couplet. By this time, the mesovortex-induced winds had begun to weaken, although severe winds at the ground continued even beyond the last analysis time (i.e., 05:59:34 UTC) presented in this study. A broad area of rotation persisted at midlevels through ~06:15 UTC, but no rotation was clearly evident on the lowest elevation scan.

7. SUMMARY AND CONCLUSIONS

A simple technique has been employed to investigate damaging wind production in bow echoes, whereby damage locations were overlaid directly onto radar images. The results of the present study provide clear observational evidence that, in addition to descending rear inflow at the bow-echo apex, low-level mesovortices within bow echoes can produce damaging straight-line winds at the ground. The various bow echo events are summarized as follows.

In four of the five damage analyses presented as part of this study, a midlevel RIJ was present in the trailing stratiform precipitation region of the bow-shaped convective system. Largely, descending rear inflow at the bow-echo apex produced F0-intensity wind damage. The squall line bow echo on 4-5 July 2003, with a horizontal scale in excess of 100 km, produced only localized F0 damage areas with embedded F1-intensity wind damage, as revealed by ground surveys. In the case of the bow echo on 5-6 July 2003, RIJ/apex winds produced widespread F0-intensity wind damage across eastern Nebraska and western Iowa. Yet, the most intense wind damage was born of another mechanism (namely mesovortex-induced winds).

Damage analyses of the “Emerson” and “Shelby” bow echoes on 10 June 2003 suggest a possible relationship between the horizontal scale of a bow echo and the strength of the RIJ. Both of these systems rapidly evolved from tornadic supercells into intense cell bow echoes. While damaging wind production was confined to the formative stages of these systems, the distributions of damage locations were rather dense. Further, the “Shelby” bow echo produced a narrow swath of F1-intensity wind damage approximately 10 km in length.

The results of this study, as well as a parallel investigation of a squall-line bow echo that caused considerable damage in southwestern Illinois on 10 June 2003 (Atkins et al. 2004, this volume), also have substantiated the mesovortex-damaging wind paradigm put forth by Trapp and Weisman (2003). When present, mesovortices in BAMEX bow echo events were associated with the most intense wind damage. The MCS on 30-31 May 2003 over central Indiana lacked an intense RIJ, but strong surface winds (F0-intensity) were driven for a brief time (approximately 3 volume scans) by a shallow, broad mesovortex located in the active leading-line convection. Otherwise, the parent system was not associated with severe winds as it continued to propagate across central Indiana, as gauged by *Storm Data* reports.

The bow echo on 5-6 July 2003 produced widespread F0-intensity wind damage across eastern Nebraska and western Iowa, but the most damaging straight-line winds occurred in association with two mesovortices in the bowing system. Notably, the second bow-echo vortex produced an approximately 15-km-long swath of F1-intensity wind damage (over western Iowa), which was embedded within a primary (F0-intensity) damage area over 50 km in length!

While the present study has evidenced the severe weather potential of low-level mesovortices within bow echoes, the question remains whether mesovortex-induced winds can be anticipated in an operational setting. In the present study, the “spinup” of these mesovortices occurred rather rapidly (a couple of volume scans) and hence would limit warning lead time. It should be noted that Atkins et al. (2004a) found tornadic mesovortices within the QLCS on 29 June 1998 (over Iowa and Illinois) to be stronger and longer-lived than nontornadic mesovortices. Thus, it would seem that the formulation of a definitive means by which to distinguish severe/non-severe mesovortices awaits examination of mesovortex structure within future bow echo events.

Acknowledgements: The research results presented herein were supported by the National Science Foundation under Grants ATM-023344 (RJT and DMW) and ATM-0233178 (NTA).

8. REFERENCES

Atkins, N. T., J. M. Arnott, R. W. Pryzbylinski, R. A. Wolf, and B. D. Ketcham, 2004a: Vortex structure and evolution within bow echoes. Part I: Single-Doppler and damage analysis of the 29 June 1998 Derecho. *Mon. Wea. Rev.*, in press.

Atkins, N. T., C. Bouchard, R. W. Pryzbylinski, R. J. Trapp, G. K. Schmocker, 2004b: Damaging surface wind mechanisms within the 10 June 2003 Saint Louis bow echo event during BAMEX. Preprints, *22th Conf. on Severe Local Storms*, Boston, MA, Amer. Meteor. Soc.

Cotton, W. R., R. McAnelly, and C. Wolff, 2003: Mesoscale vortices and mesocyclones as precursors to derechoes. Preprints, *10th Conf. on Mesoscale Processes*, Seattle, WA, Amer. Meteor. Soc.

Davis, C. and co-authors, 2004: The Bow Echo and MCV Experiment (BAMEX): Observations and opportunities. *Bull. Amer. Meteor. Soc.*, in press.

Fujita, T. T., 1978: Manual of downburst identification for project Nimrod. Satellite and Mesometeorology Research Paper 156, Dept. of Geophysical Sciences, University of Chicago, 104 pp. [NTIS PB-286048.]

Funk, T. W., K. E. Darmofal, J. D. Kirkpatrick, V. L. Dewald, R. W. Pryzbylinski, G. K. Schmocker, and Y.-J Lin, 1999: Storm reflectivity and mesocyclone evolution associated with the 15 April 1994 squall line over Kentucky and southern Indiana. *Wea. Forecasting*, **14**, 976-993.

Hamilton, R. E., 1970: Use of detailed intensity radar data in mesoscale surface analysis of the 4 July 1969 storm in Ohio. Preprints, *14th Conf. on Radar Meteorology*, Tucson, AZ, Amer. Meteor. Soc., 339-342.

Jorgensen, D. P., and B. F. Smull, 1993: Mesovortex circulations seen by airborne Doppler radar within a bow-echo mesoscale convective system. *Bull. Amer. Meteor. Soc.*, **74**, 2146-2157.

Lakshmanan, V., 2002: WDSS-II: An extensible, multi-source meteorological algorithm development interface. Preprints, *21st Conference on Severe Local Storms*, San Antonio, TX, Amer. Meteor. Soc., 134-137.

Miller, D. J. and R. H. Johns, 2000: A detailed look at extreme wind damage in derecho events. Preprints, *20th Conf. on Severe Local Storms*, Orlando, FL, Amer. Meteor. Soc., 52-55.

Nolen, R. H., 1959: A radar pattern associated with tornadoes. *Bull. Amer. Meteor. Soc.*, **40**, 277-279.

Orlanski, I., 1975: A rational subdivision of scales for atmospheric processes. *Bull. Amer. Meteor. Soc.*, **56**, 527-530.

Oye, R., C. Mueller, and S. Smith, 1995: Software for radar translation, visualization, editing, and interpolation. Preprints, *29th Conf. on Radar Meteorology*, Vail, CO, Amer. Meteor. Soc., 359-361.

Pryzbylinski, R. W., G. K. Schmocker, and Y.-J. Lin, 2000: A study of storm and vortex morphology during the 'intensifying stage' of severe wind mesoscale convective systems. Preprints, *20th Conf. on Severe Local Storms*, Amer. Meteor. Soc., Orlando, FL, 173-176.

Rinehart, R. E., 1978: On the use of ground targets for radar reflectivity factor calibration checks. *J. Appl. Meteor.*, **17**, 1342-1350.

Schmocker, G. K., R. W. Pryzbylinski, and E. N. Rasmussen, 2000: The severe bow echo event of 14 June 1998 over the mid-Mississippi Valley region: A case of vortex development near the intersection of a preexisting boundary and a convective line. Preprints, *20th Conf. on Severe Local Storms*, Amer. Meteor. Soc., Orlando, FL, 169-172.

Smull, B. F., and R. A. Houze, Jr., 1987: Rear inflow in squall lines with trailing stratiform precipitation. *Mon. Wea. Rev.*, **115**, 2869-2889.

Stumpf, G., T. Smith, and A. Gerard, 2002: The multiple-radar severe storm analysis program for WDSS-II. Preprints, *21st Conference on Severe Local Storms*, San Antonio, TX, Amer. Meteor. Soc., 138-141.

Trapp, R. J., and M. L. Weisman, 2003: Low-level mesovortices within squall lines and bow echoes. Part II: Their genesis and implications. *Mon. Wea. Rev.*, **131**, 2804 – 2823.

Wakimoto, R. M., and P. G. Black, 1994: Damage survey of Hurricane Andrew and its relationship to the eyewall. *Bull. Amer. Meteor. Soc.*, **75**, 189-200.

_____, and N. T. Atkins, 1996: Observations on the origins of rotation: the Newcastle tornado during VORTEX 94. *Mon. Wea. Rev.*, **124**, 384-407.

Weisman, M. L., and R. J. Trapp, 2003: Low-level mesovortices within squall lines and bow echoes. Part I: Overview and dependence on environmental shear. *Mon. Wea. Rev.*, **131**, 2779-2803.

Witt, A., M. D. Eilts, G. J. Stumpf, E. D. Mitchell, J. T. Johnson, and K. W. Thomas, 1998: Evaluating the performance of the WSR-88D severe storm detection algorithms. *Wea. Forecasting*, **13**, 513-518.

Wolf, R. A., 2000: Characteristics of circulations associated with the 29 June 1998 derecho in eastern Iowa. Preprints, *20th Conf. on Severe Local Storms*, Orlando, FL, Amer. Meteor. Soc., 56-59.

Table 1. Information regarding damage surveys conducted during BAMEX

Date(s)	Mission	Mode	Location	Aerial Survey	Ground Survey
30-31 May	IOP 3	Long-lived MCS	Wingate, IN	Atkins	Trapp
10 June	IOP 7A	Cell Bow Echo	Emerson, NE	Atkins	Wheatley
10 June	IOP 7A	Cell Bow Echo	Shelby, NE	Atkins	Wheatley
4-5 July	IOP 17	Squall-line Bow Echo	Indiana/Ohio	NONE	Trapp, Wheatley
5-6 July	IOP 18	Squall-line Bow Echo	Nebraska/Iowa	Atkins, Wakimoto	Atkins, Wakimoto

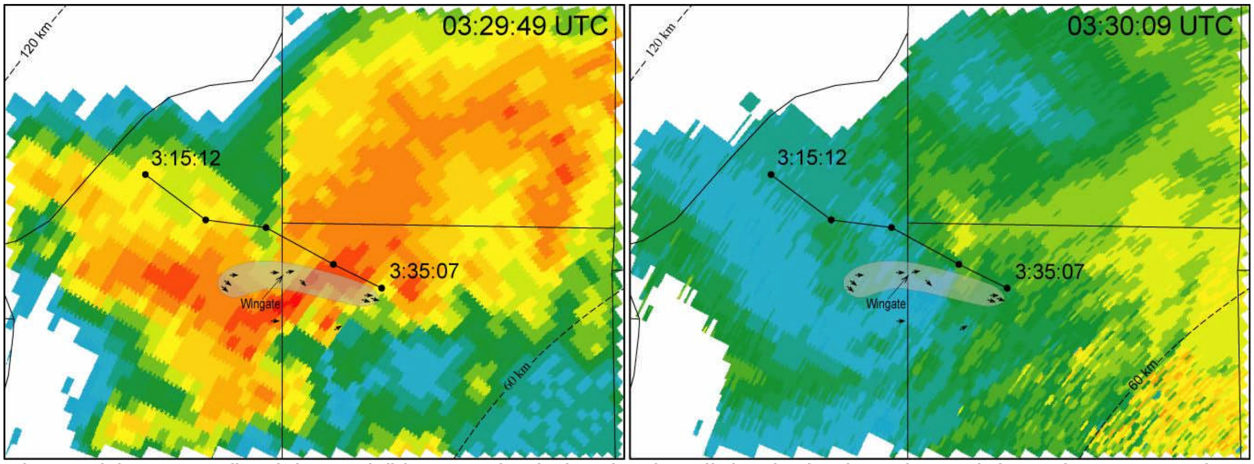

Fig. 1. (a) Base reflectivity and (b) ground-relative (GR) radial velocity (0.5-degree) from the KIND radar at 03:29:49 and 03:30:09 UTC 31 May 2003, respectively. Damage analysis over central Indiana. Solid polyline shows the track of vortex core (as determined by WDSS-II).

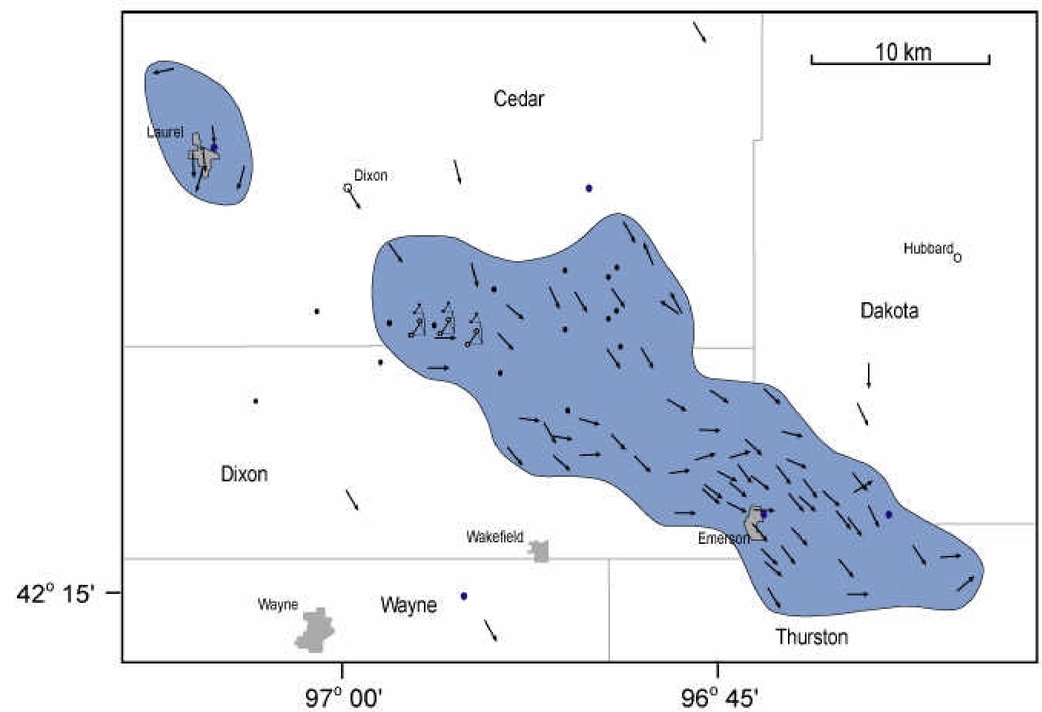

Fig. 2. Damage analysis performed for the "Emerson" bow echo on 10 June 2003 over northeast Nebraska (F0 = light blue, F1 = dark blue). Blue polymarkers show locations of Storm Data wind reports.

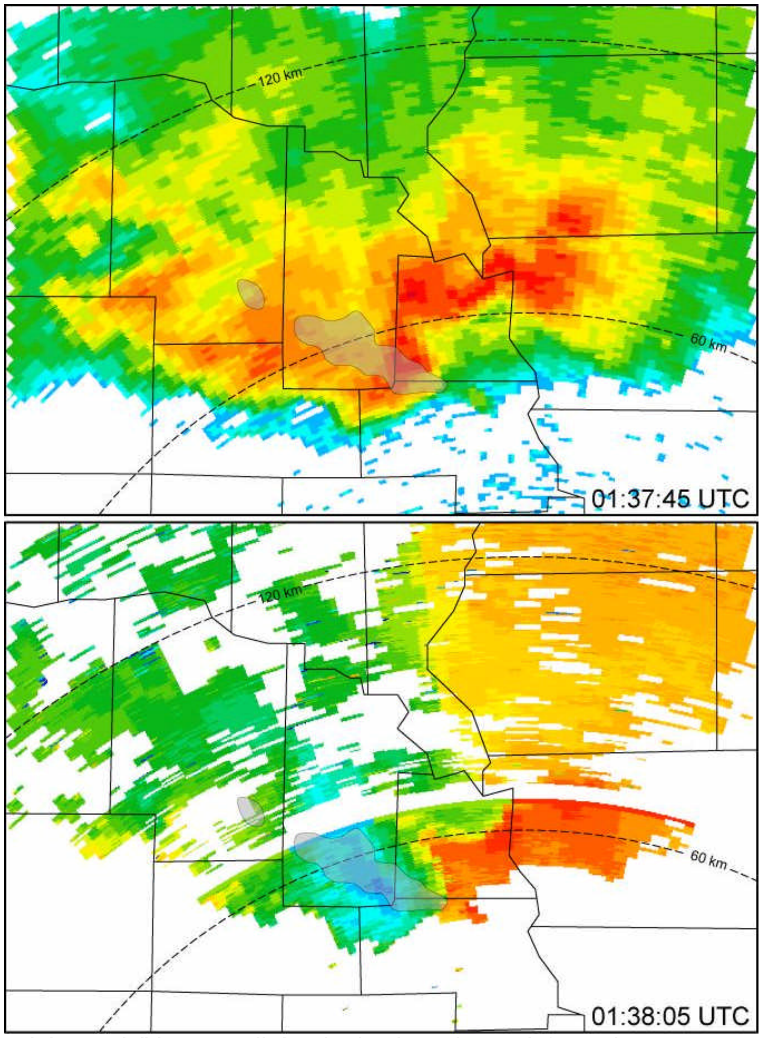

Fig. 3. (a) Base reflectivity and (b) GR radial velocity (0.5-degree) from the KOAX radar at 01:37:45 and 01:38:05 UTC 10 June 2003, respectively. Damage analysis over northeastern Nebraska.

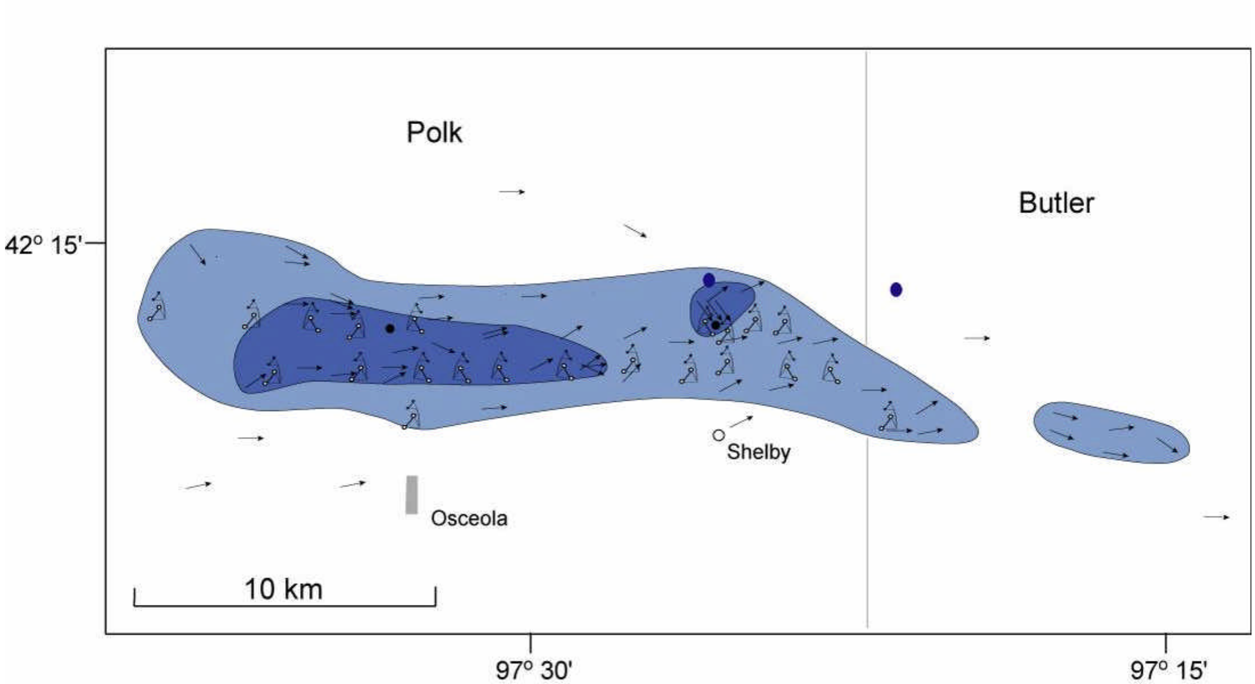

Fig. 4. Damage analysis performed for the "Shelby" bow echo on 10 June 2003 over east-central Nebraska.

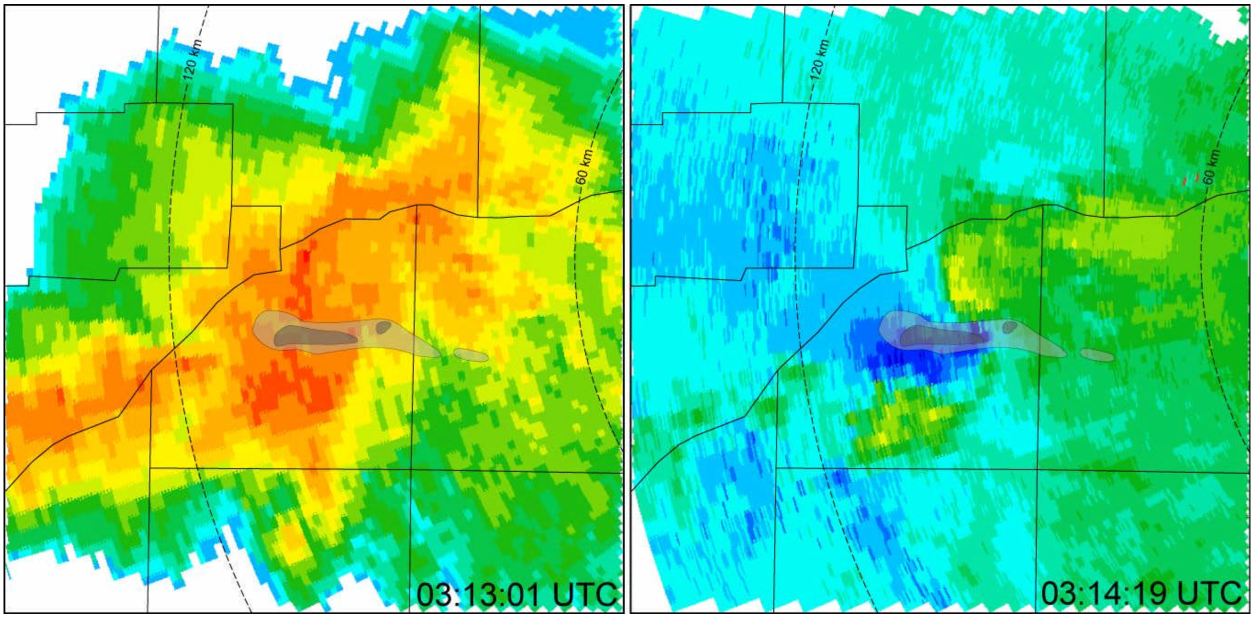

Fig. 5. Same as Fig. 3, except at (a) 03:13:01 and (b) 03:14:19 UTC 10 June 2003. (The maximum of rear-to-front flow behind the convective line is shown on the 2.4-degree elevation surface.) Damage analysis over east-central Nebraska.

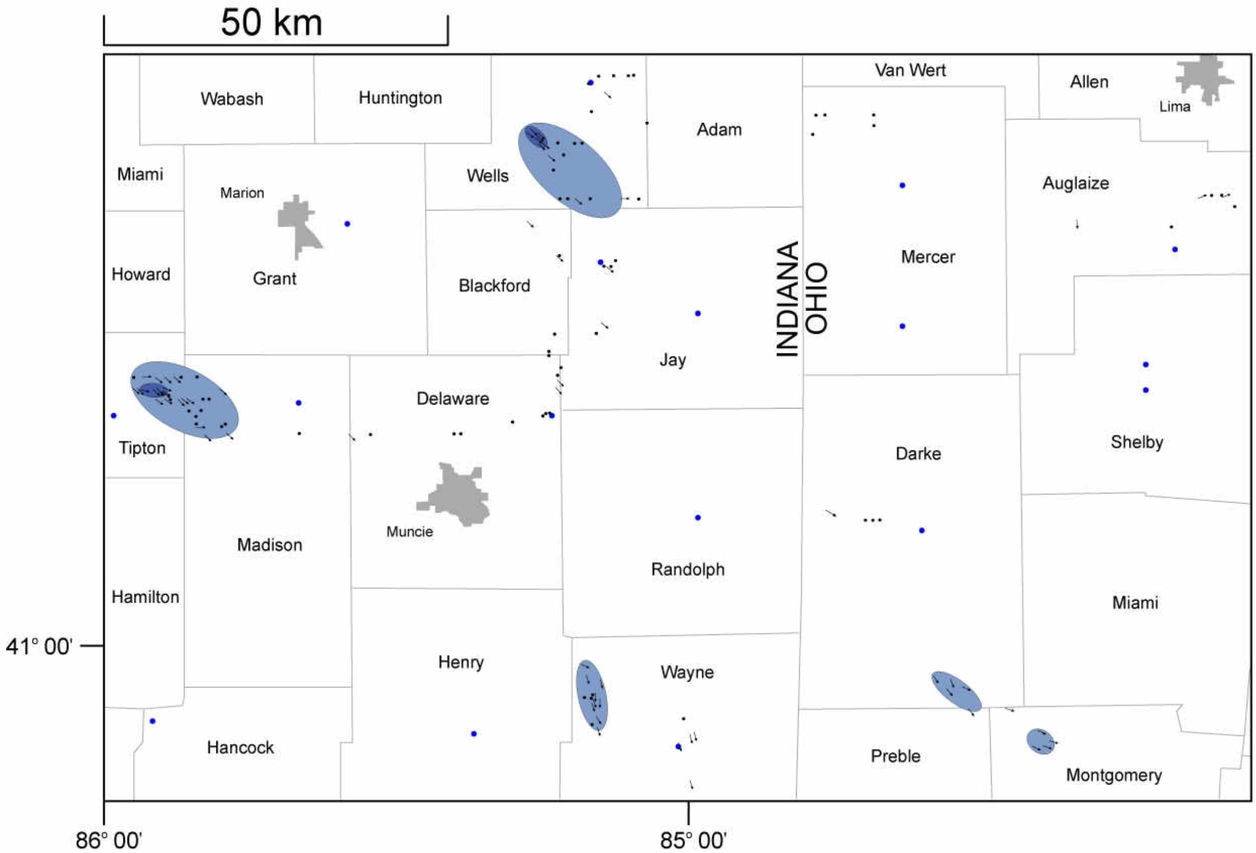

Fig. 6. Damage analysis performed for the bow echo on 4-5 July 2003 over central Indiana and eastern Ohio.

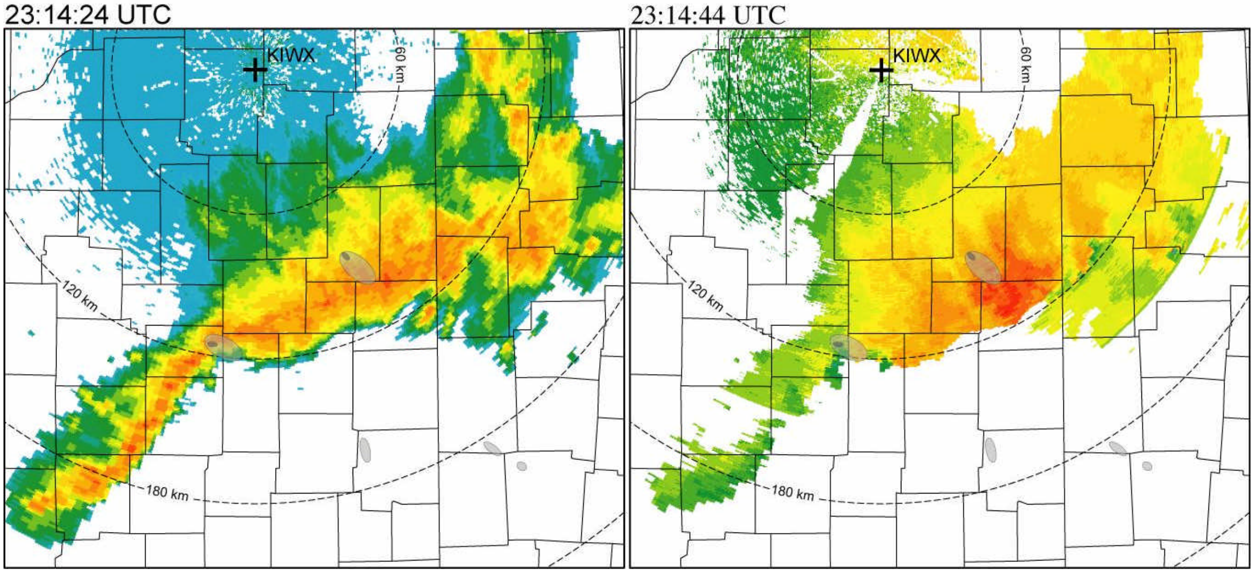

Fig. 7. Same as Fig. 3, except at (a) 23:14:24 and (b) 23:14:44 UTC 4 July 2003. Damage analysis over central Indiana and eastern Ohio.

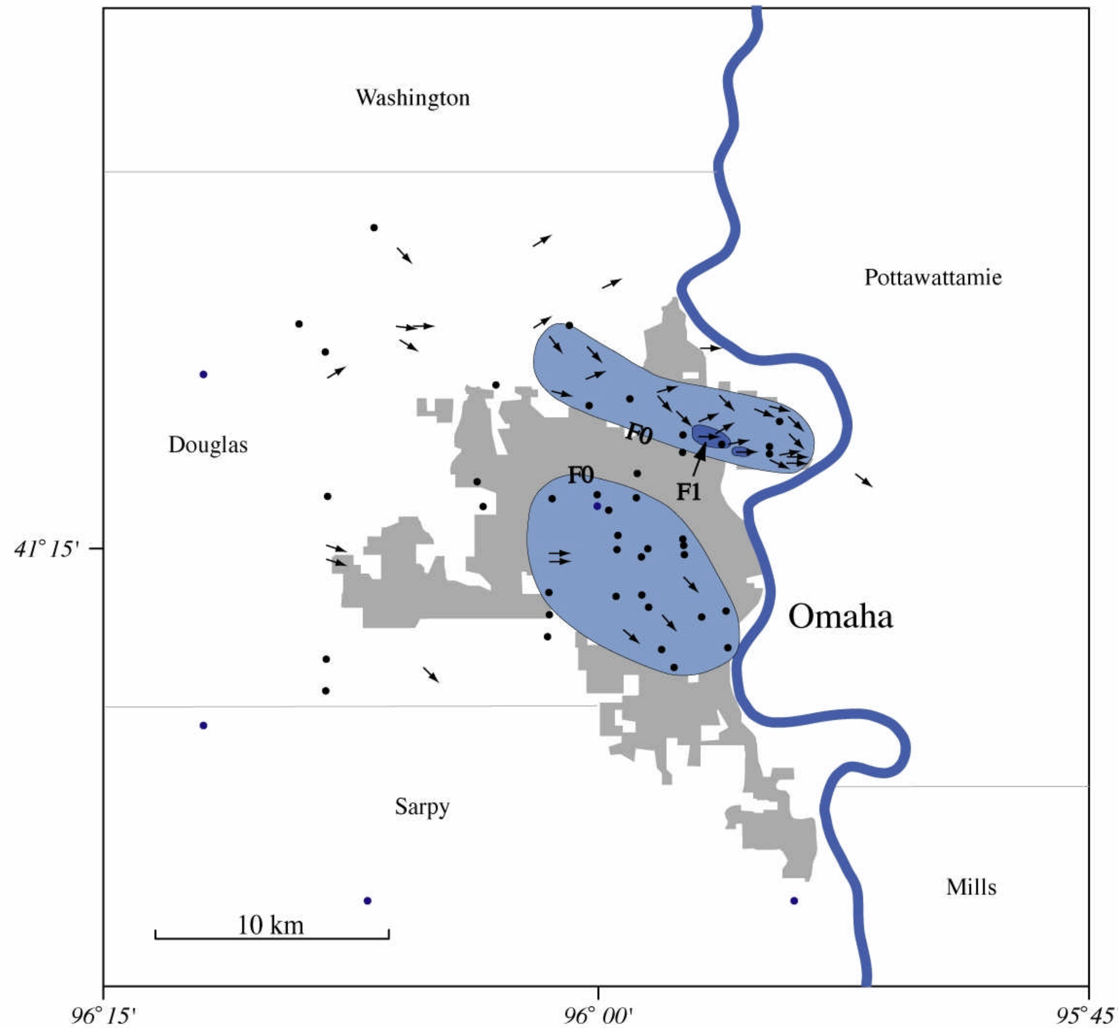

Fig. 8. Damage analysis performed for the bow echo on 5-6 July 2003 over Omaha metropolitan area.

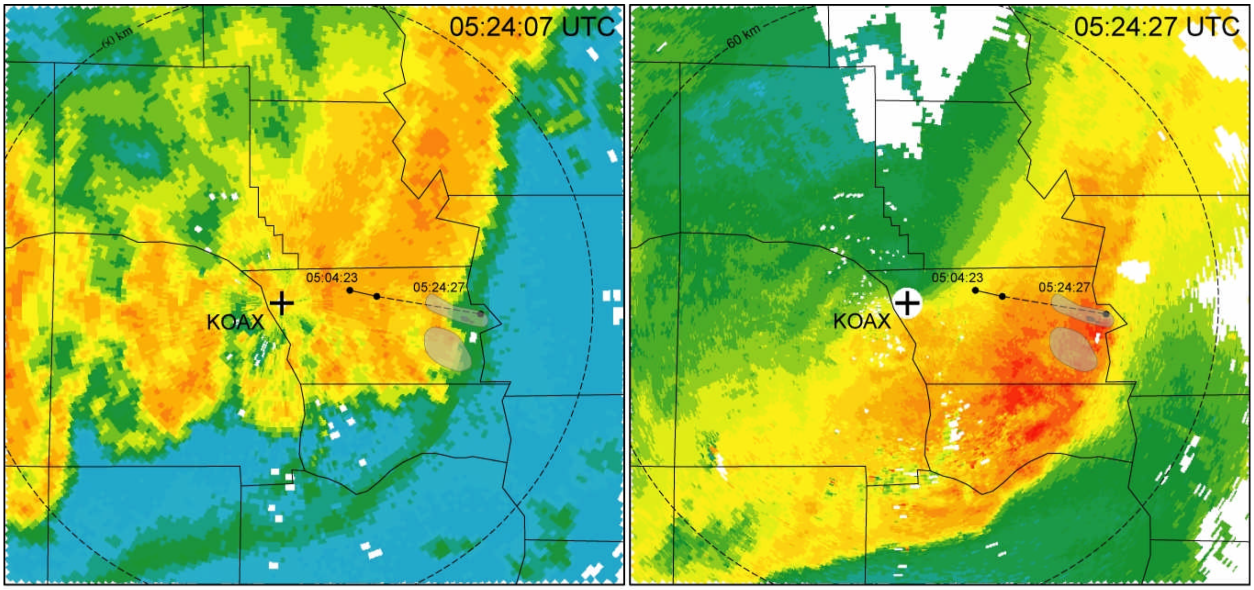

Fig. 9. Same as Fig. 1, except at (a) 05:24:07 and (b) 05:24:27 UTC 6 July 2003. Damage analysis over Omaha metropolitan area

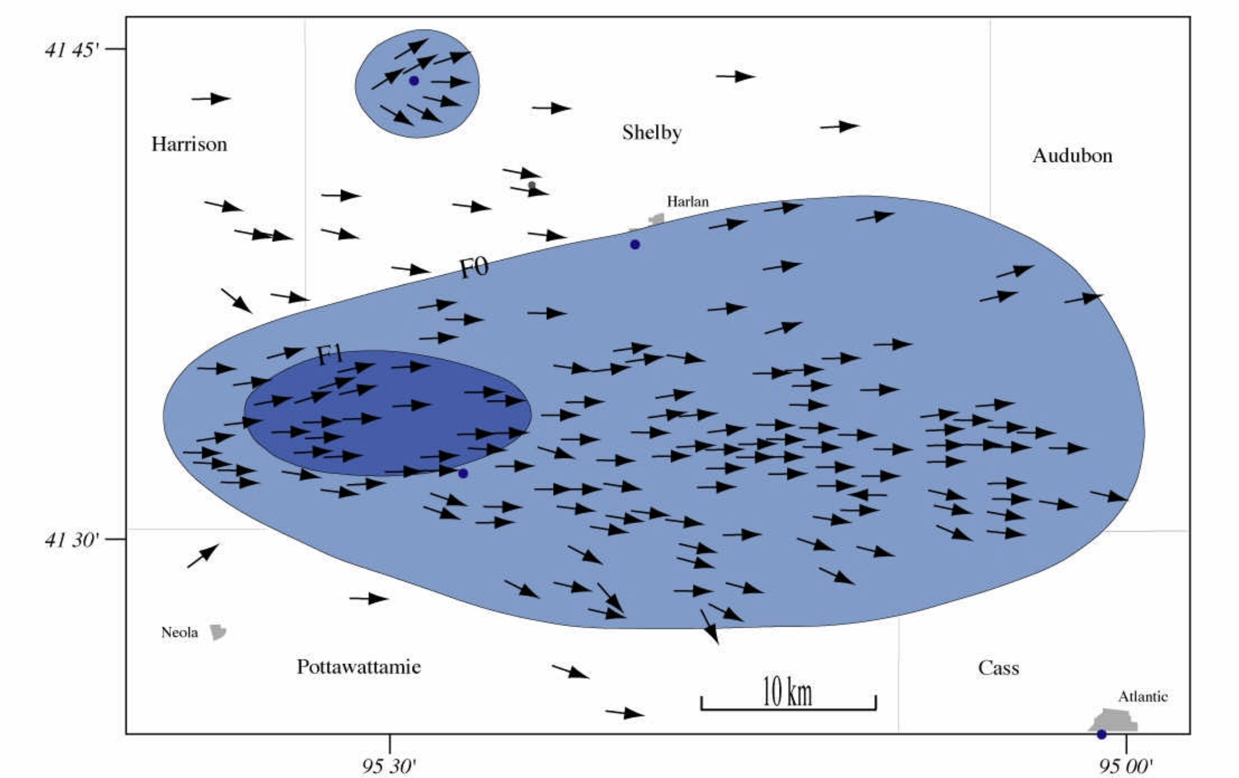

Fig. 10. Damage analysis performed for the bow echo on 5-6 July 2003 over western Iowa.

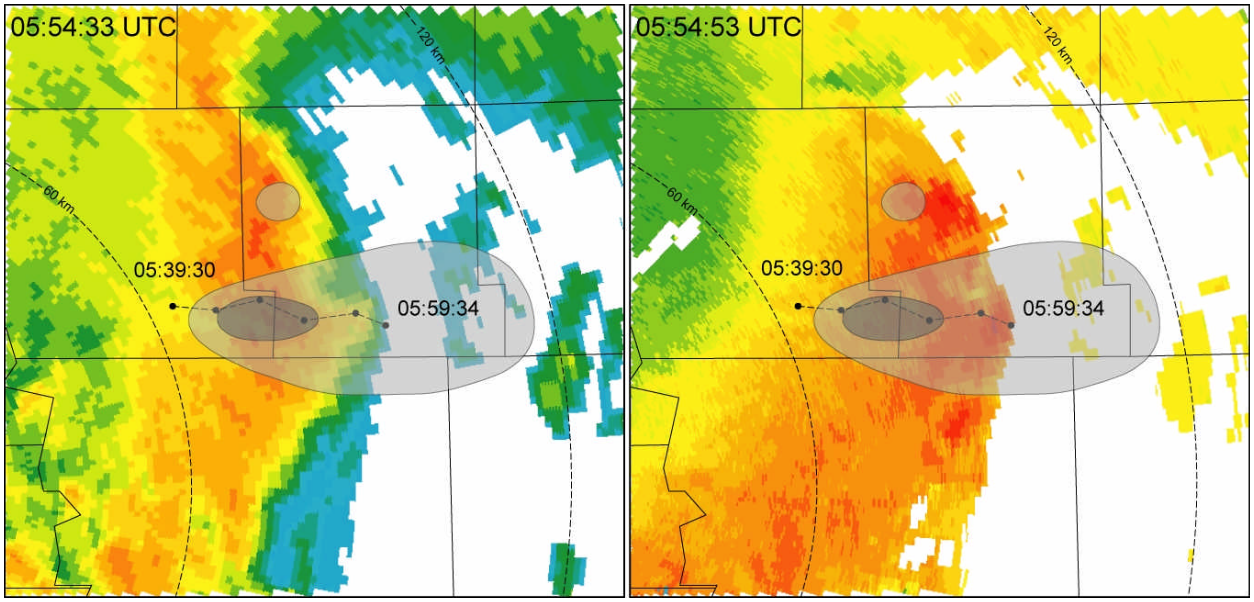

Fig. 11. Same as Fig. 1, except at (a) 05:54:33 and (b) 05:54:53 UTC 6 July 2003. Damage analysis over western Iowa.